Journal of Hazardous Materials Advances 19 (2025) 100790

Contents lists available at ScienceDirect

Journal of Hazardous Materials Advances

journal homepage: www.elsevier.com/locate/hazadv

Relative biodistribution and accumulation of carbonaceous nanoparticles inside the murine and human kidney

Leen Rasking [a], Kenneth Vanbrabant [a], Maartje Vangeneugden [a], Thessa Van Pee [a], Flemming R. Cassee [b,c], Hannelore Bové [d], Katrien De Vusser [e,f], Michelle Plusquin [a], Tim S. Nawrot [a,g,*]

[a] Centre for Environmental Sciences, Hasselt University, Diepenbeek, Belgium
[b] Centre for Sustainability, Environment and Health, National Institute for Public Health and the Environment, RIVM, Bilthoven, The Netherlands
[c] Institute for Risk Assessment Sciences (IRAS), Utrecht University, Utrecht, The Netherlands
[d] Faculty of Sciences, Hasselt University, Diepenbeek, Belgium
[e] Nephrology and Kidney Transplantation, University Hospital Leuven, Leuven, Belgium
[f] Department of Microbiology and Immunology, Leuven University, Leuven, Belgium
[g] Department of Public Health and Primary Care, Environment and Health Unit, Leuven University, Leuven, Belgium

ARTICLE INFO

Keywords:
Air pollution
Fine particulate matter
Black carbon
Carbonaceous nanoparticles
Kidney
Biodistribution
Immunofluorescence

ABSTRACT

Background: Epidemiological and toxicological studies underscore the adverse health effects of combustion-derived particles, such as carbonaceous nanoparticles (CNPs), which translocate to various organs, including the kidneys. Given the kidneys play a crucial role in filtering toxins, CNP accumulation may pose a risk to renal function. We investigated CNP biodistribution in murine and human kidney tissue to assess potential impacts on kidney health.

Methods: In the controlled murine model, wild-type C57BL/6J mice were exposed to CNPs through whole-body exposure. Human kidney tissue was analyzed without prior knowledge of exposure history. CNPs in kidney tissue were detected using femtosecond-pulsed illumination and quantified via a peak-finding algorithm. Renal components – the glomerulus, proximal and distal tubules, and blood vessels – were visualized through immunofluorescence. Colocalization of CNPs with renal structures was quantified using the Just Another Colocalization Plugin. Structural differences were evaluated using Kruskal-Wallis tests.

Results: CNPs were detected in all investigated renal structures of both mouse and human kidneys, providing direct evidence of their translocation. The relative distribution was comparable between species, with no statistically significant differences in colocalization ($q > 0.05$). The percentages of CNPs in mice *vs.* humans colocalized with glomeruli (1.46 % vs. 1.91 %), proximal tubules (13.43 % vs. 16.10 %), distal tubules (2.72 % vs. 3.25 %), and blood vessels and capillaries (4.16 % vs. 5.21 %).

Conclusions: Proximal tubules exhibited the highest relative CNP accumulation in both species. This aligns with research linking environmental pollutants, such as black carbon, to decreased tubular kidney function, suggesting proximal tubule involvement in particle processing.

1. Background

Epidemiological studies have already established the importance of combustion-derived particles, a subcomponent of ambient fine particulate matter ($PM_{2.5}$, particles < 2.5 μm in diameter), as an important component in driving the adverse effects observed after PM exposure (Nemmar et al., 2002, Van Berlo et al., 2014). Various health effects have been reported, including cardiovascular diseases (Upadhyay et al., 2014), pulmonary diseases (André et al., 2006, Saleh et al., 2019), and even effects on pregnancy outcomes and birth (Janssen et al., 2017, Zhu et al., 2015). In an urban setting, ultrafine PM mainly consists of carbonaceous nanoparticles (CNPs), generated from *e.g.*, incomplete combustion processes. (Janssen et al., 2012) Moreover, toxicological studies have already demonstrated the health hazards of inhaled $PM_{2.5}$ and different components of $PM_{2.5}$ may induce different health effects. Moreover, CNPs, including black carbon (BC), are generally not viewed as directly toxic components; however, they are thought to serve as

* Corresponding author at: Centre for Environmental Sciences, Hasselt University, Agoralaan Building D, BE-3590 Diepenbeek, Belgium.
E-mail address: tim.nawrot@uhasselt.be (T.S. Nawrot).

https://doi.org/10.1016/j.hazadv.2025.100790
Received 14 April 2025; Received in revised form 1 June 2025; Accepted 18 June 2025
Available online 18 June 2025

Glossary

AQP-1	aquaporin-1
BC	black carbon
CALB	calbindin
CI	confidence interval
CNP	carbonaceous nanoparticle
JACoP	just another colocalization plugin
KIM-1	kidney injury molecule-1
SMA	smooth muscle actin
SYNPO	synaptopodin
UFP^C	ultrafine carbonaceous nanoparticle

universal carriers of harmful substances in the air (Janssen et al., 2012, Janssen et al., 2011).

Nemmar et al. (2002) were the first to demonstrate that ultrafine carbonaceous nanoparticles can promptly translocate into the systemic circulation upon inhalation, potentially reaching distant organs. Later studies, in both rodents and humans, confirmed this phenomenon under real-life environmental exposure conditions, showing the translocation and deposition of CNPs in various organ systems, including the placenta (Bové et al., 2019), the brain (Van Berlo et al., 2014, Vanbrabant et al., 2024), the liver (LeFevre et al., 1982, Bongaerts et al., 2023), spleen (LeFevre et al., 1982), and kidneys (Rasking et al., 2023). The kidneys hold an essential function in filtering the blood of excess fluid and waste; receiving approximately 25 % of cardiac output, they filter the blood up to 60 times per day. (Pizzorno, 2015) Nevertheless, certain toxins may present challenges during the removal process. For instance, substances like cadmium can prove difficult to be eliminated from the blood circulation and excreted into the urine as it can accumulate in the kidney and causes damage. (Honda et al., 2010, Johri et al., 2010, Ma et al., 2023, Thomas et al., 2009) As a result, these toxins tend to accumulate in the kidneys over time, increasing the risk of kidney damage as their concentration rises. (Pizzorno, 2015) Therefore, accumulated deposition of CNPs into the kidney may influence kidney function over time. We have previously demonstrated the translocation of these CNPs into the urine of healthy children (Saenen et al., 2017) and kidneys of transplant recipients (Rasking et al., 2023), along with the subsequent decline in tubular function associated with CNP exposure (Rasking et al., 2023).

However, it is not clear in which structural renal component(s) these CNPs accumulate, which may provide insight into the adverse effects and excretion mechanism(s) of CNPs by the kidneys. Here, we investigated the biodistribution and accumulation of CNPs in kidney tissue derived from mice exposed to ultrafine carbonaceous particles (UFP^C) and in kidney surveillance biopsy tissue derived from kidney transplant recipients one-year post-transplantation.

2. Methods

2.1. Mouse exposure and kidney processing

Wild-type C57BL/6J OlaHsd mice were exposed to CNPs at a target concentration of 450 μg/m³ during gestation and postnatally, or to HEPA-filtered clean air (sham). Mice underwent a total of sixteen exposure days: four days during gestation, eight days in early postnatal life, and four days in adulthood. A detailed description of this study and its exposure periods is provided elsewhere. (Vanbrabant et al., 2024) On average, the actual mass concentration was 430 ± 59 μg/m³ for prenatal exposure on GD 8, 9, 16, and 17 and 442 ± 82 μg/m³ for postnatal exposure on PND 4–7 and 10–13, with an average continuously measured particle number concentration of $5.1 \times 10^6 \pm 0.4 \times 10^6$ particles per cc and $4.6 \times 106 \pm 0.4 \times 106$ particles per cc for the prenatal and postnatal exposure periods, respectively.

While the CNP concentrations used in our murine exposure model exceed typical ambient levels encountered in European urban environments (e.g., 3.4 ± 2.3 μg/m³ to a maximum of 5.2 ± 2.8 μg/m³ (Savadkoohi et al., 2023)), they were intentionally selected to enable detectable tissue-level accumulation within a short experimental timeframe, as described previously (Vanbrabant et al., 2024). The 4-hour exposure duration approximates a daily average of ~70 μg/m³, representing a proof-of-concept concentration. To support visualization and quantification of biodistribution, this elevated dose was used to ensure measurable nanoparticle retention within the limited window of developmental exposure in mice. This approach facilitates the evaluation of CNP localization during early-life vulnerability without aiming to mimic real-world exposure levels directly.

Thirty-six days after the last exposure, the six-month-old mice (PND 181 to 182) were euthanized; kidney tissues were perfused with a sterile PBS solution prior to organ harvesting, dorsally sectioned, fixed in 4 % paraformaldehyde for a minimum of 16h and embedded in paraffin. Kidney tissue was sectioned at 4 μm using a microtome (Leica Microsystems, United Kingdom), floated onto charged glass slides (SuperFrost Plus, Fisher Scientific, USA), and dried overnight at 37 °C. For this study, 10 kidney tissue samples were selected based on their CNP load in kidney tissue. All experimental procedures were conducted in accordance with EU Directive 2010/63/EU for animal experiments and were approved by the local ethical committee of Hasselt University for animal experiments (ID 202148B and 201864A1).

2.2. Human kidneys

Kidney allograft surveillance ('protocol') biopsies ($n = 10$) were obtained approximately 12 months post-transplantation. Routine allograft protocol biopsies are performed by a trained physician at the time of transplantation, and 3, 12, and 24 months after transplantation, in addition to clinical indication biopsies. Here, surveillance biopsies, obtained one year post-transplantation, were fixed in 4 % paraformaldehyde and embedded in paraffin prior to sectioning at 4 μm. Written informed consent was obtained from all patients for the use of their kidney biopsy tissue for research purposes following routine medical care. Secondary use of these samples was approved by the Ethical Committee of the University Hospital of Leuven (S64649).

The Flemish study cohort had a mean age of 53.20 ± 13.15 years, with 60 % male participants and a mean body mass index (BMI) of 21.26 ± 2.90 kg/m². The average time interval between transplantation and biopsy sampling was 391.9 ± 29.35 days. At the time of biopsy, the participants exhibited a mean estimated glomerular filtration rate (eGFR) of 46.11 ± 14.38 mL/min/1.73 m².

2.3. Immunofluorescence

Relative biodistribution of CNPs in structural renal components was evaluated by staining glomeruli, proximal tubules, distal tubules, and blood vessels at least in duplicate (human samples) or triplicate (rodent samples). For biodistribution analysis, 4 μm thick kidney paraffin sections were deparaffinized in 100 % xylene and rehydrated in a graded ethanol series (100 % to 50 %). Antigen retrieval was performed using sodium citrate buffer (10 mM, pH 6), where sections were cooked in the microwave for 15 mins before allowing them to cool to room temperature. After blocking non-specific binding sites with protein block (10 % goat serum, 50062Z, Life Technologies, USA) for 60 mins, tissue sections were probed with antibodies against i) synaptopodin to visualize glomeruli (SYNPO, 1:400, 21064-1-AP, ProteinTech, China), ii) aquaporin-1 to visualize proximal tubules (AQP1, 1:1,500, 20333-1-AP, ProteinTech), iii) calbindin to visualize distal tubules (CALB, 1:1,500, 14479-1-AP, ProteinTech), and iv) smooth muscle actin to visualize blood vessels and capillaries (SMA, 1:1,000, ab124964, Abcam, United Kingdom) overnight at 4 °C. After washing, the tissue sections were

incubated with an Alexa Fluor® 488 conjugated goat-anti-rabbit secondary antibody (1:500, A11008, Invitrogen, USA) for two hours at room temperature. All antibodies were diluted in 10 % protein block/1x PBS. As a nuclear counterstain, SYTO^{TM} 61 Red (1:1,500, S11343, Invitrogen, USA) was employed.

2.4. Biodistribution of black carbon and colocalization imaging

Alexa Fluor®-labeled renal structures and SYTO^{TM} 61 Red-labeled nuclei were excited using an Argon laser (488 nm) and a He-Ne laser (633 nm), respectively. Band-pass filters of 490 – 600 and 650 – 750 nm were used for filtering the emission signal from the labeled renal structures and nuclei, respectively. CNPs present in kidney tissue were detected using a sensitive and specific technique based on the non-incandescence-related white light generation of the carbonaceous nanoparticles under femtosecond-pulsed illumination, as described in detail elsewhere. (Bové et al., 2019, Rasking et al., 2023, Saenen et al., 2017, Bové et al., 2016) The microscope was equipped with a two-photon femtosecond-pulsed laser (150 fs, 80 MHz, MaiTai DeepSee, Spectra-Physics, USA) tuned to a central wavelength of 810 nm with a ± 3.5 mW radiant power on average at the sample, employing a 20x/0.8 (Aprochromat, Carl Zeiss) objective. The number of CNPs in the obtained images is determined using a peak-finding algorithm, which counts pixels above a threshold value. Fingerprinting and validation of CNPs in human kidney tissue has been performed previously. (Rasking et al., 2023)

For the mouse kidney tissue, 10 tile scans of 2 × 2 of paraffin-embedded kidney tissue, sectioned at 4 μm, were collected at room temperature using a Zeiss LSM880 (Carl Zeiss, Jena, Germany) confocal microscope. For the human kidney biopsy tissue, the whole biopsy specimen was captured in 2 × 2 tile scans for the proximal and distal tubules, and single images of each structure were obtained for all the blood vessels and glomeruli present in the biopsy sample. Manders' overlap coefficients, the percentage of CNPs associated with the labeled renal structures, were calculated using the Fiji Just Another Colocalization Plugin (JACoP) in Fiji (ImageJ 1.54f, Open source software, http://fiji.sc/Fiji). (Schindelin et al., 2012) Prior to analysis, a threshold was set to the estimated background value for each renal structure. The colocalization coefficient was defined as the percentage of CNPs that overlap with the labeled renal structures, reflecting the fraction of CNPs within these structures relative to the total CNP signal in the image. Channel registration was corrected using TetraSpeck™ Fluorescent Microspheres (T7279, Invitrogen, USA) and manually aligned to overlap. Furthermore, obtained coefficients are not dependent on the relative intensities of each channel and cross-talk between the channels was found to be negligible (Bongaerts et al., 2021).

For the murine study, both the exposed group and the control group were analyzed. As no significant differences were observed in particle distribution across renal structures, results were not reported separately. Instead, the focus was placed on particle localization.

For the SMA visualization in human kidney biopsy tissue, we omitted approximately half of the acquired images (45.5 %) due to the occurrence of fibrotic SMA-positive tissue in the sample, potentially rendering false-positive results in regards to CNP bioaccumulation in blood vessels and capillaries.

2.5. Statistics

Data are represented as mean (95 % confidence interval [CI]) and analyzed using the commercially available GraphPad Prism software (GraphPad Prism 8, GraphPad Software Inc., USA) and RStudio software (RStudio 2022.02.3, USA). Differences between the different renal structures were evaluated using Kruskal-Wallis test with multiple testing accounted for using the false discovery rate (FDR). Differences were considered statistically significant at $q < 0.05$.

3. Results

The accumulation of CNPs was observed in all of the four investigated renal structures for both species (Fig. 1 and Supplemental Fig. 1). In the mouse study, in general, 1.46 % (95 % CI: 0.94 to 1.97) of CNPs were observed in the glomeruli, 13.43 % (95 % CI: 11.60 to 15.27) were found in the proximal tubules, 2.72 % (95 % CI: 1.57 to 3.87) in the distal tubules, and 4.16 % (95 % CI: 2.77 to 5.55) of CNPs were detected in the blood vessels and capillaries (Fig. 2A), based on the percentage of CNPs colocalized with each structure. Significant differences were observed between the proximal tubules and glomeruli, blood vessels and capillaries, and distal tubules ($q < 0.0001$). A borderline significant trend was observed between the blood vessels and glomeruli ($q = 0.0535$) and distal tubules ($q = 0.0801$); however, no significant difference could be observed between the glomeruli and distal tubules ($q = 0.789$).

Similar results were obtained for the biodistribution of CNPs in kidney surveillance biopsies one year post-transplantation. Here, we observed 1.91 % (95 % CI: 0.54 to 3.28) of CNPs in the glomeruli, 16.10 % (95 % CI: 10.90 to 21.30) in the proximal tubules, 3.25 % (95 % CI: 2.12 to 4.37) in the distal tubules, and 5.21 % (95 % CI: 3.07 to 7.34) of CNPs overlapped with the blood vessels and capillaries (Fig. 2B). When considering the proximal tubules, significant differences were observed with glomeruli ($q < 0.0001$), blood vessels and capillaries ($q = 0.0043$), and distal tubules ($q < 0.0001$). All other investigated renal structures showed significant differences, except when comparing the blood vessels and capillaries and the distal tubules ($q = 0.2415$).

When addressing the renal structures separately, there was no difference observed in the percentage of particle colocalizing with *e.g.*, proximal tubules, between mice and humans (*e.g.*, proximal tubules: $q = 0.946$).

4. Discussion

In this study, we investigated the relative biodistribution and accumulation of carbonaceous nanoparticles inside kidney tissue in a murine model and in human kidney biopsy tissue. Previous research has already indicated that toxins, such as cadmium, may accumulate in the kidney over time upon repeated exposure. (Pizzorno, 2015) Earlier, we showed that higher BC load in kidney tissue of kidney transplant recipients one year post-transplantation is associated with increased acute tubular damage, as indicated by increased levels of KIM-1. (Rasking et al., 2023) Additionally, we demonstrated that gestational particulate air pollution exposure influenced newborn glomerular kidney function. (Rasking et al., 2024) Our study reveals that carbonaceous nanoparticles predominantly accumulate in the proximal tubules of kidney tissue, with lesser amounts found in blood vessels and capillaries, distal tubules, and glomeruli, providing insights into the potential localization and extent of damage observed in previous studies. This conclusion is based on semi-quantitative colocalization analysis using Manders' coefficient, which measures the relative overlap of CNP signals with nephron segment-specific markers. While this approach does not provide absolute quantification, it reliably indicates a higher relative localization in proximal tubules compared to other renal structures. These findings were consistently observed in both a murine model and human kidney biopsy tissue samples, providing important spatial insights into potential sites of CNP interaction within the kidney and laying the groundwork for future studies to explore functional consequences in more detail.

In mammals, the kidney is responsible for the elimination of metabolic wastes from the body. The glomerulus filters out waste, excess ions, and water, creating the filtrate that enters the tubules. Subsequently, the proximal tubules reabsorb approximately 65 to 80 % of the glomerular filtrate to achieve homeostasis for water and electrolytes in the body. Further reabsorption takes place in the distal tubules. Secretion of exogenous substances, such as toxins, from the tubular cells into the tubular lumen, is one of the most important excretory functions of

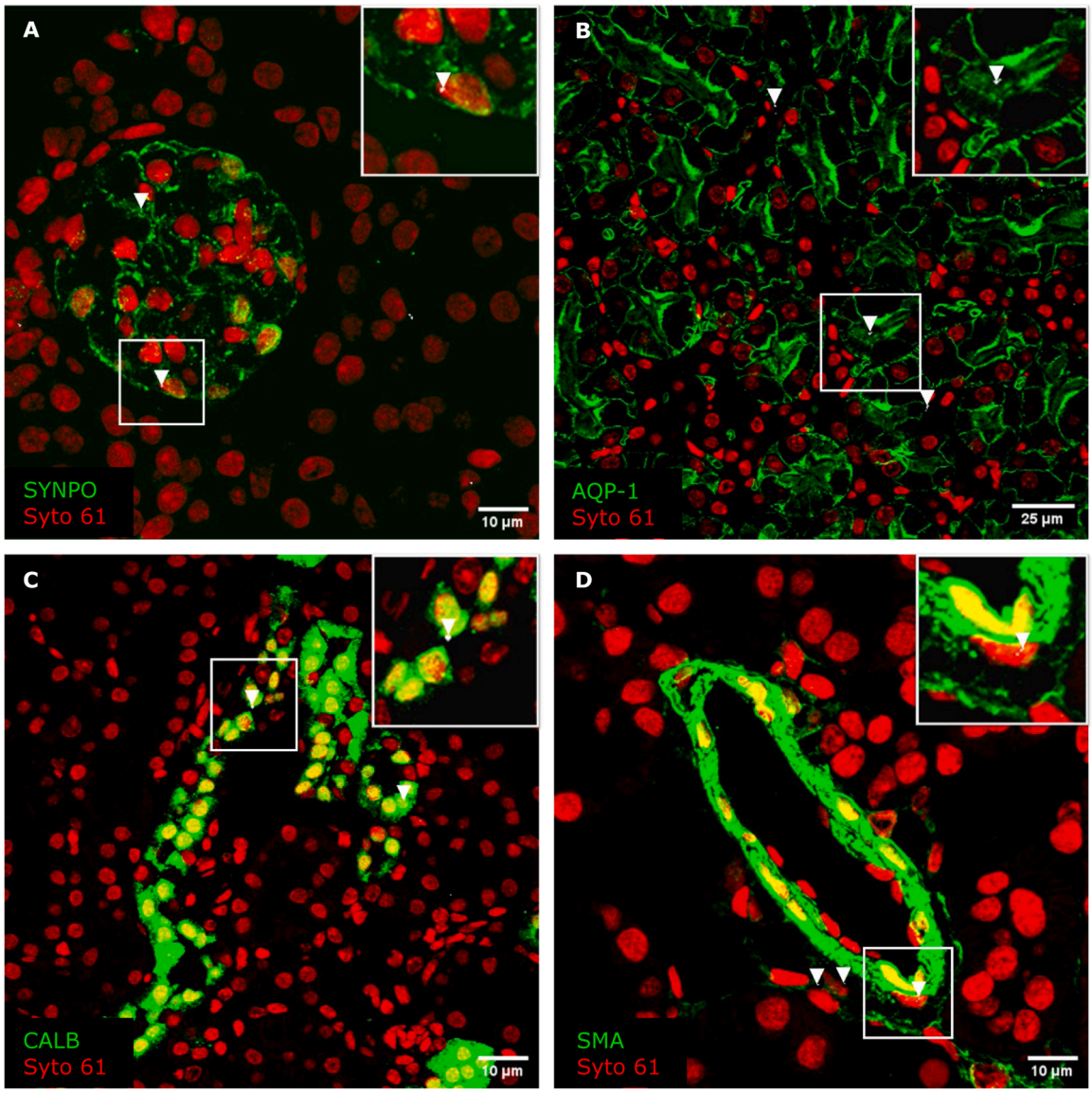

Fig. 1. CNP accumulation observed in all four investigated renal structures. (A) glomeruli (green) are stained with synaptopodin primary antibody (1:400), **(B)** proximal tubules (green) are stained with aquaporin-1 primary antibody (1:1,500), **(C)** distal tubules (green) are stained with calbindin primary antibody (1:1,500), and **(D)** blood vessels and capillaries (green) were stained with smooth muscle actin (1:1,000). Syto61 Red (red) was used as a nuclear counterstain. Carbonaceous nanoparticles are depicted with white arrowheads. Scale bar = 10 µm. ***Abbreviations***: AQP-1, aquaporin-1; CALB, calbindin; CNPs, carbonaceous nanoparticles; SMA, smooth muscle actin; SYNPO, synaptopodin.

the kidney. (Finco, 1997) However, active toxin excretion pathways have a limited capacity, and are easily saturated. (Pizzorno, 2015) Over time, the buildup of toxins may disrupt (tubular) cellular function, damage mitochondria, and generate oxidative stress, which can impair the reabsorption function of the proximal tubules and downstream cause kidney damage, proteinuria, and a decrease in overall kidney function. In addition, if the mitochondria of the kidneys aren't working well, the active excretion pathways that require ATP do not work as required. The kidneys then fail to protect themselves as toxin concentrations builds up inside the kidneys. (Pizzorno, 2015) It was already shown that particulate air pollution exposure causes increased mitochondrial oxidative DNA damage. (Gualtieri et al., 2011, Grevendonk et al., 2016)

The blood vessels and capillaries were the second most prominent sites of relative CNP accumulation in this study. This finding raises the question of whether the observed CNP accumulation arises from pre-filtration blood supply or from tubular reabsorption, leading to subsequent secretion into the bloodstream. Given the distinct afferent and efferent function of kidney blood vessels, investigating the specific localization of CNPs within these pathways could provide valuable additional insights. (Dalal et al., 2018)

Furthermore, our results show that the well-controlled UFP^C exposure during the animal study renders similar results as the heterogenous CNP exposure of the transplant recipients. Even though the two are physically and chemically distinct substances, UFP^C, such as *e.g.*, carbon black, are commonly employed to investigate effects of particulate air pollution in *in vitro* or *in vivo* settings. (Watson and Valberg, 2001) Moreover, Watson *et al.* elucidated that some CNP forms, such as *e.g.*, diesel exhaust particles, may have similar aggregate morphology as their manufactured counterparts. (Watson and Valberg, 2001) It is important to note that the exposure concentrations used in our murine model exceed typical ambient levels and were intentionally selected to enable detectable biodistribution patterns within a short experimental timeframe, rather than to replicate real-world exposure scenarios.

Overall, our findings are in line with previous work, which show that the proximal tubules are the most affected area in the kidney upon air pollution, and more importantly CNP exposure. (Rasking et al., 2023)

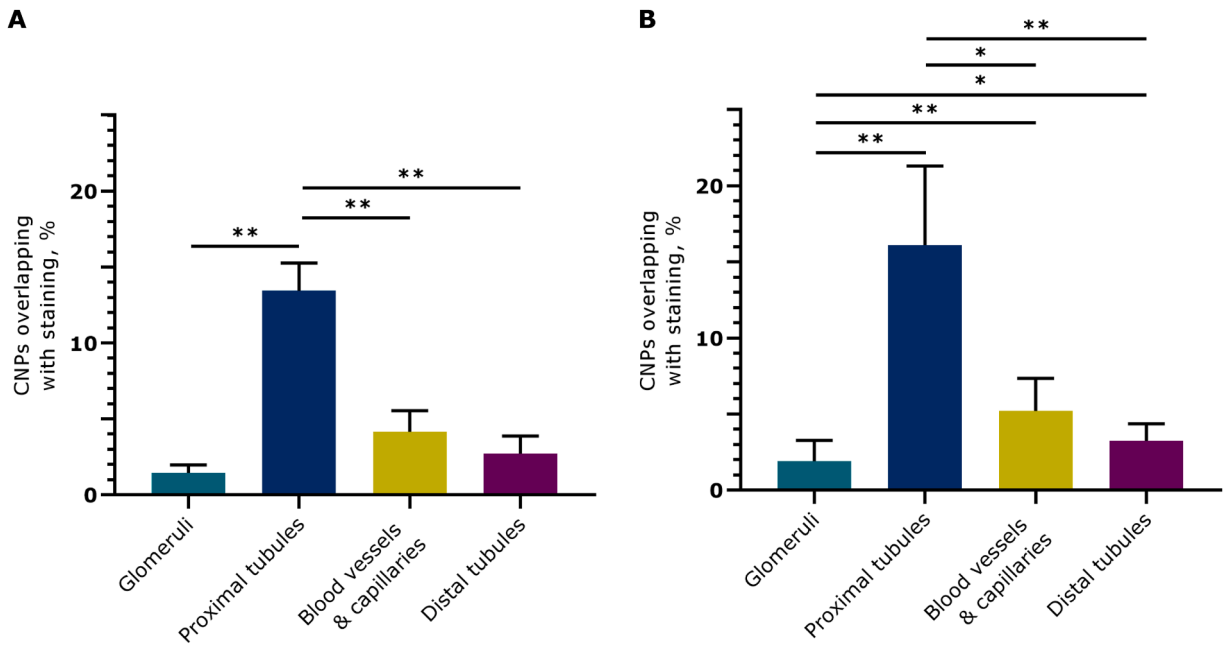

Fig. 2. Relative biodistribution in percentage of CNPs in the four investigated renal structures in kidney tissue. (A) Results of mouse kidney tissue ($n = 10$), where the most prominent site of CNP accumulation were the proximal tubules (13.43 %), followed by the blood vessels and capillaries (4.16 %), the distal tubules (2.72 %), and lastly, the glomeruli (1.46 %), and **(B)** results of the human biopsy kidney tissue ($n = 10$), where the most prominent site of CNP accumulation were the proximal tubules (16.10 %), followed by the blood vessels and capillaries (5.21 %), the distal tubules (3.25 %), and lastly, the glomeruli (1.91 %). Error bars represent the 95 % confidence interval. ** $q < 0.0001$, * $q < 0.005$.

Our study has several strengths. First, we are able to visualize and relatively quantify CNP accumulation in a label-free setting, without the need for extensive labelling, as is required with general common fluorophores. (Bové et al., 2016) Second, our results are validated through cross-species analysis, revealing similar patterns of CNP accumulation in renal structures across both murine and human models, reinforcing the translational relevance of our results. Lastly, a key strength of this study is the use of pure UFP^C in the mouse model, while the human study examines complex CNPs derived from ambient air pollution, which are not considered 'pure' and consist of a carbon core with additional compounds bound to its shell such as *e.g.*, benzene or polycyclic hydrocarbons; this dual approach allows us to assess particle accumulation across a spectrum of controlled and real-world exposure conditions, respectively.

While our findings shed light on the localization of carbonaceous nanoparticles in the kidney, it is important to emphasize that this study focused specifically on their biodistribution rather than on functional or pathological outcomes. Although kidney health is influenced by numerous factors—such as inflammation (Keller et al., 2007, Puthumana et al., 2021), fibrosis (Mansour et al., 2017), or systemic toxicity (Prozialeck and Edwards, 2010)—which can be assessed through biomarkers or histopathological evaluation (Miettinen et al., 2014), these were outside the scope of the current work. Our aim was to provide spatial insight into where these particles accumulate, serving as a foundational step toward understanding potential downstream effects. At present, it remains unclear whether the levels of CNP accumulation we observed in the kidney—and in particular in the proximal tubules—reach toxicological thresholds that impair renal function. However, the fact that proximal tubules showed the highest relative CNP burden load is notable, especially given previous studies in transplant recipients showing that increased CNP load is associated with elevated KIM-1 levels, a biomarker of proximal tubular dysfunction. (Rasking et al., 2023) These findings underscore the need for future studies to establish exposure thresholds at which particle burden translates into functional toxicity, ideally by integrating biodistribution data with histopathology and markers of renal function, such as eGFR, creatinine, or blood urea nitrogen. Furthermore, the human kidney biopsy tissue samples are not derived from generally healthy individuals, as kidney transplant recipients are on immunosuppressive medication to prevent graft rejection, potentially increasing their susceptibility to environmental toxins. (Chang et al., 2021) However, similar results were observed in healthy C57BL/6 mice in this study, suggesting that CNP accumulation may occur regardless of baseline health status.

5. Conclusion

Our findings reveal that the proximal tubules exhibit the highest percentage of CNP colocalization among renal structures in both mouse and human kidney tissue samples. This observation aligns with prior research, indicating that proximal tubules are a key site of pollutant-induced damage and dysfunction due to their exposure to environmental pollutants, such as CNPs. Moreover, the consistency of CNP accumulation patterns between murine and human models support the translational relevance of these results.

Funding

The authors acknowledge funding from the Special Research Fund (BOF) from Hasselt University granted to L.R. (BOF20DOC15) and funding from the Research Foundation Flanders (FWO) granted to K.V. (G059219). Additionally, the animal study was supported by the European Union's Horizon 2020 research and innovation program under grant agreement No. 814978 (TUBE). BOF nor FWO nor TUBE had no role in the design, conduct, and preparation of the manuscript.

Data sharing

The data used in the findings of this study are not publicly available, but are available upon reasonable request from the corresponding author (T.S.N.).

CRediT authorship contribution statement

Leen Rasking: Writing – review & editing, Writing – original draft, Visualization, Validation, Project administration, Methodology, Investigation, Funding acquisition, Formal analysis, Data curation, Conceptualization. **Kenneth Vanbrabant:** Writing – review & editing, Validation, Methodology, Investigation, Funding acquisition, Data curation, Conceptualization. **Maartje Vangeneugden:** Writing – review & editing, Investigation. **Thessa Van Pee:** Writing – review & editing, Investigation. **Flemming R. Cassee:** Writing – review & editing, Supervision, Resources, Investigation. **Hannelore Bové:** Writing – review & editing, Methodology, Conceptualization. **Katrien De Vusser:** Supervision, Resources. **Michelle Plusquin:** Writing – review & editing, Validation, Supervision, Methodology, Formal analysis, Data curation. **Tim S. Nawrot:** Writing – review & editing, Writing – original draft, Supervision, Project administration, Methodology, Funding acquisition, Formal analysis, Data curation.

Declaration of competing interest

H.B. and T.S.N. declare that aspects of the work are subject of a patent application (Method for detecting or quantifying carbon black and/or black carbon particles, US20190025215A1) filed by Hasselt University (Hasselt, Belgium) and KU Leuven (Leuven, Belgium). The remaining authors declare no competing interests. None of the funding agencies had a role in the design and conduct of the study, in the collection, analysis and interpretation of the data, or in the preparation, review, or approval of the manuscript.

Disclaimer: the content has not gone through all the steps in the RIVM quality assurance process. Therefore, the contents of this manuscript cannot be referred to as “the opinion or position” of RIVM.

Acknowledgements

The authors wish to thank and acknowledge Mr. J. Boere, Mr. E. Duistermaat, and Mr. P. Fokkens with the assistance and the execution of the exposure experiments. Furthermore, the authors wish to thank Roel P.F. Schins and his colleagues with the assistance in setting up the exposure and feedback. Additionally, the authors wish to acknowledge and thank Mr. R. Braeken for the fixation and paraffin embedding of mouse kidney tissue samples and the AOMC for the microscopy support. The authors wish to thank Ms. J. De Loor for her aid with collection and transportation of kidney biopsy tissue. The authors also thank the centers of the Leuven Collaborative Group for Renal Transplantation, as well as the clinicians, lab technicians, surgeons, nursing staff, and patients in the study.

Supplementary materials

Supplementary material associated with this article can be found, in the online version, at doi:10.1016/j.hazadv.2025.100790.

Data availability

Data will be made available on request.

References

Nemmar, A., Hoet, P.M., Vanquickenborne, B., Dinsdale, D., Thomeer, M., Hoylaerts, M., et al., 2002. Passage of inhaled particles into the blood circulation in humans. Circulation 105 (4), 411–414.

Van Berlo, D., Hullmann, M., Wessels, A., Scherbart, A., Cassee, F., Gerlofs-Nijland, M., et al., 2014. Investigation of the effects of short-term inhalation of carbon nanoparticles on brains and lungs of c57bl/6j and p47phox−/− mice. Neurotoxicology 43, 65–72.

Upadhyay, S., Stoeger, T., George, L., Schladweiler, M.C., Kodavanti, U., Ganguly, K., et al., 2014. Ultrafine carbon particle mediated cardiovascular impairment of aged spontaneously hypertensive rats. Part. Fibre Toxicol. 11, 1–18.

André, E., Stoeger, T., Takenaka, S., Bahnweg, M., Ritter, B., Karg, E., et al., 2006. Inhalation of ultrafine carbon particles triggers biphasic pro-inflammatory response in the mouse lung. Eur. Respir. J. 28 (2), 275–285.

Saleh, Y., Antherieu, S., Dusautoir, R., Y Alleman, L., Sotty, J., De Sousa, C., et al., 2019. Exposure to atmospheric ultrafine particles induces severe lung inflammatory response and tissue remodeling in mice. Int. J. Environ. Res. Public Health 16 (7), 1210.

Janssen, B.G., Saenen, N.D., Roels, H.A., Madhloum, N., Gyselaers, W., Lefebvre, W., et al., 2017. Fetal thyroid function, birth weight, and in utero exposure to fine particle air pollution: a birth cohort study. Environ. Health Perspect. 125 (4), 699–705.

Zhu, X., Liu, Y., Chen, Y., Yao, C., Che, Z., Cao, J., 2015. Maternal exposure to fine particulate matter (PM 2.5) and pregnancy outcomes: a meta-analysis. Environmental Science and Pollution Research 22, 3383–3396.

Janssen, N.A., Gerlofs-Nijland, M.E., Lanki, T., Salonen, R.O., Cassee, F., Hoek, G., et al., 2012. Health Effects of Black Carbon: World Health Organization. Regional Office for Europe.

Janssen, N.A., Hoek, G., Simic-Lawson, M., Fischer, P., Van Bree, L., Ten Brink, H., et al., 2011. Black carbon as an additional indicator of the adverse health effects of airborne particles compared with PM10 and PM2. 5. Environ. Health Perspect. 119 (12), 1691–1699.

Bové, H., Bongaerts, E., Slenders, E., Bijnens, E.M., Saenen, N.D., Gyselaers, W., et al., 2019. Ambient black carbon particles reach the fetal side of human placenta. Nat. Commun. 10 (1), 3866.

Vanbrabant, K., Van Dam, D., Bongaerts, E., Vermeiren, Y., Bové, H., Hellings, N., et al., 2024. Accumulation of ambient black carbon particles within key memory-related brain regions. JAMA Netw. Open 7 (4) e245678-e.

LeFevre, M.E., Green, F.H., Joel, D.D., Laqueur, W., 1982. Frequency of black pigment in livers and spleens of coal workers: correlation with pulmonary pathology and occupational information. Hum. Pathol. 13 (12), 1121–1126.

Bongaerts, E., Nawrot, T.S., Wang, C., Ameloot, M., Bové, H., Roeffaers, M.B., et al., 2023. Placental-fetal distribution of carbon particles in a pregnant rabbit model after repeated exposure to diluted diesel engine exhaust. Part. Fibre Toxicol. 20 (1), 20.

Rasking, L., Koshy, P., Bongaerts, E., Bové, H., Ameloot, M., Plusquin, M., et al., 2023. Ambient black carbon reaches the kidneys. Environ. Int. 177, 107997.

Pizzorno, J., 2015. The kidney dysfunction epidemic, part 1: causes. Integrative Medicine: A Clinician’s Journal 14 (6), 8.

Honda, R., Swaddiwudhipong, W., Nishijo, M., Mahasakpan, P., Teeyakasem, W., Ruangyuttikarn, W., et al., 2010. Cadmium induced renal dysfunction among residents of rice farming area downstream from a zinc-mineralized belt in Thailand. Toxicol. Lett. 198 (1), 26–32.

Johri, N., Jacquillet, G., Unwin, R., 2010. Heavy metal poisoning: the effects of cadmium on the kidney. Biometals 23, 783–792.

Ma, Y., Yue, C., Sun, Q., Wang, Y., Gong, Z., Zhang, K., et al., 2023. Cadmium exposure exacerbates kidney damage by inhibiting autophagy in diabetic rats. Ecotoxicol. Environ. Saf. 267, 115674.

Thomas, L.D., Hodgson, S., Nieuwenhuijsen, M., Jarup, L., 2009. Early kidney damage in a population exposed to cadmium and other heavy metals. Environ. Health Perspect. 117 (2), 181–184.

Saenen, N.D., Bové, H., Steuwe, C., Roeffaers, M.B., Provost, E.B., Lefebvre, W., et al., 2017. Children’s urinary environmental carbon load. A novel marker reflecting residential ambient air pollution exposure? Am. J. Respir. Crit. Care Med. 196 (7), 873–881.

Vanbrabant, K., Rasking, L., Vangeneugden, M., Bové, H., Ameloot, M., Vanmierlo, T., et al., 2024. Impact on murine neurodevelopment of early-life exposure to airborne ultrafine carbon nanoparticles. Part. Fibre Toxicol. 21, 51.

Savadkoohi, M., Pandolfi, M., Reche, C., Niemi, J.V., Mooibroek, D., Titos, G., et al., 2023. The variability of mass concentrations and source apportionment analysis of equivalent black carbon across urban Europe. Environment international. 178, 108081.

Bové, H., Steuwe, C., Fron, E., Slenders, E., D’Haen, J., Fujita, Y., et al., 2016. Biocompatible label-free detection of carbon black particles by femtosecond pulsed laser microscopy. Nano Lett. 16 (5), 3173–3178.

Schindelin, J., Arganda-Carreras, I., Frise, E., Kaynig, V., Longair, M., Pietzsch, T., et al., 2012. Fiji: an open-source platform for biological-image analysis. Nat. Methods 9 (7), 676–682.

Bongaerts, E., Aengenheister, L., Dugershaw, B.B., Manser, P., Roeffaers, M.B., Ameloot, M., et al., 2021. Label-free detection of uptake, accumulation, and translocation of diesel exhaust particles in ex vivo perfused human placenta. J. Nanobiotechnol. 19, 1–13.

Rasking, L., Van Pee, T., Vangeneugden, M., Renaers, E., Wang, C., Penders, J., et al., 2024. Newborn glomerular function and gestational particulate air pollution. EBio Med 107.

Finco, DR., 1997. Kidney function. Clinical Biochemistry of Domestic Animals. Elsevier, pp. 441–484.

Gualtieri, M., Øvrevik, J., Mollerup, S., Asare, N., Longhin, E., Dahlman, H-J, et al., 2011. Airborne urban particles (Milan winter-PM2. 5) cause mitotic arrest and cell death: effects on DNA, mitochondria, AhR binding and spindle organization. Mutation Res./Fundam. Molec. Mechanisms Mutag. 713 (1-2), 18–31.

Grevendonk, L., Janssen, B.G., Vanpoucke, C., Lefebvre, W., Hoxha, M., Bollati, V., et al., 2016. Mitochondrial oxidative DNA damage and exposure to particulate air pollution in mother-newborn pairs. Environ. Health 15, 1–8.

Dalal R, Bruss ZS, Sehdev JS. Physiology, renal blood flow and filtration. 2018.

Watson, A.Y., Valberg, PA., 2001. Carbon black and soot: two different substances. AIHAJ-Am. Indust. Hygiene Associat. 62 (2), 218–228.

Bové, H., Steuwe, C., Fron, E., Slenders, E., D'Haen, J., Fujita, Y., et al., 2016. Biocompatible label-free detection of carbon black particles by femtosecond pulsed laser microscopy. Nano Lett. 16 (5), 3173–3178.
Keller, C., Odden, M., Fried, L., Newman, A., Angleman, S., Green, C., et al., 2007. Kidney function and markers of inflammation in elderly persons without chronic kidney disease: the health, aging, and body composition study. Kidney Int. 71 (3), 239–244.
Puthumana, J., Thiessen-Philbrook, H., Xu, L., Coca, S.G., Garg, A.X., Himmelfarb, J., et al., 2021. Biomarkers of inflammation and repair in kidney disease progression. J. Clin. Invest. 131 (3).
Mansour, S.G., Puthumana, J., Coca, S.G., Gentry, M., Parikh, CR., 2017. Biomarkers for the detection of renal fibrosis and prediction of renal outcomes: a systematic review. BMC nephrology 18, 1–13.
Prozialeck, W.C., Edwards, JR., 2010. Early biomarkers of cadmium exposure and nephrotoxicity. Biometals 23, 793–809.
Miettinen, J., Helin, H., Pakarinen, M., Jalanko, H., Lauronen, J., 2014. Histopathology and biomarkers in prediction of renal function in children after kidney transplantation. Transpl. Immunol. 31 (2), 105–111.
Chang, S-H, Merzkani, M., Murad, H., Wang, M., Bowe, B., Lentine, K.L., et al., 2021. Association of ambient fine particulate matter air pollution with kidney transplant outcomes. JAMA Netw. Open 4 (10) e2128190-e.